Journal of Optoelectronics and Advanced Materials Vol. 6, No. 4, December 2004, p. 1243 - 1253

THE COMPLETE ELECTRICAL EQUIVALENT CIRCUIT OF A DOUBLE HETEROJUNCTION LASER DIODE USING SCATTERRING PARAMETERS

M. S. Ozyazici*

University of Gaziantep, Electrical and Electronics Eng. Dept., 27310 Gaziantep, Turkey

In this work, the theory and experimentation involved in a complete electrical characterization of a commercially available semiconductor laser diode, the Hitachi HLP-1400 are described. The intrinsic electrical equivalent circuit of the laser diode is obtained from the small signal ac solution of the coupled rate equations which describe the interplay between the injected carrier and photon densities in the active region of the laser diode about the quiescent point.

(Received July 16, 2003; accepted after revision November 29, 2004)

Keywords: Laser diode, Scattering parameters, Electrical equivalent circuit

1 Introduction

The commercially available laser diode has an important application in information technology due to the fact that its highly coherent light output can be modulated to carry coded information at a high density and speed along, say, a fiber optic cable[1,2].

For the most efficient use, the modulation response characteristics of the laser diode must be exhaustively studied to find the optimum operating conditions. As device-circuit interactions will act to in°uence the response, it is not feasible to approach this problem solely from pure laser diode theory. The modulation response of the laser diode has generally been determined by solving the rate equations numerically [3,4].

This method does not take into account the influence of the package parasitics and device-circuit interactions on the modulation response. An alternative method is to use a circuit analysis based on the complete electrical circuit model of the conventional double heterostructure lasers [5-9] or quantum-well lasers [10-18], which represents a more logical choice of semiconductor laser technology for integrated optoelectronic circuits. The latter approach takes into account the package parasitics and device-circuit interaction. The complete electrical equivalent circuit is an electrical model of the complete working laser assembly which will, if designed correctly, give us an idea of the modulation response for practical applications and the maximum modulation rate that is possible for the laser diode and package/parasitics system. The circuit model can also be used to determine the impedance characteristic of the laser diode. The impedance characteristic of the laser diode is necessary for matching the laser impedance to a transmission line in order to eliminate the reflected wave due to mismatch and to increase the rf current injection to the laser diode. The complete circuit model can give us an idea how the modulation bandwidth of the laser diode can be increased by careful design of the laser diode chip and the package.

Information relating to electrical networks at high frequency is obtainable from scattering, or s-parameters. These are the complex reflection and transmission coefficients of an electrical network measured at a specified port with other ports in specified conditions. With a knowledge of the equivalent circuit's layout, the s-parameters will enable us to assign values to each of the network elements and so obtain the modulation response and impedance information we require.

* Corresponding author: sadi@gantep.edu.tr

2. Mathematical model

The complete equivalent circuit of a laser diode can be separated into two parts. The first part represents the intrinsic electrical equivalent circuit of the laser chip itself. The second part is the electrical equivalent circuit of the package including the major parasitic elements. The elements of the intrinsic laser equivalent circuit are derived from the coupled rate equations which describe the interplay between the injected carrier and photon densities in the active region of the laser diode.

The coupled single-mode rate equations are given by [19]

$$\frac{dN_e}{dt} = \frac{1}{qad} - A(N_e - N_{om})N_{ph} - \frac{N_e}{\tau_s} \tag{1}$$

$$\frac{dN_{ph}}{dt} = A(N_e - N_{om})N_{ph} - \frac{N_{ph}}{\tau_{ph}} + \beta\frac{N_e}{\tau_s} \tag{2}$$

where N_{ph} is the photon density, N_e is the electron density, q is the electronic charge, d is the thickness of the active region, a is the area of the diode contact stripe, I is the injected current, N_{om} is the minimum electron density required to obtain a positive gain, A is a constant related to the stimulated emission process, τ_s is the spontaneous emission lifetime, τ_{ph} is the photon lifetime and β is the fraction of the spontaneous emission that is coupled to the lasing mode. The above equations assume that the inversion is homogenous and the gain is linear in the difference between N_e and N_{om}.

In order to obtain the electrical model of the laser diode, one must relate the carrier density as a function of the junction voltage. For AlGaAs devices, it is given by

$$N_e = N_i \, exp\frac{qV}{2kT} \tag{3}$$

where N_i is the intrinsic carrier density and V is the junction voltage.

By using the method described in detail by Tucker [5,6], the small-signal ac solution of Equation (1) and Equation (2) with the inclusion of Equation (3) about the quiescent point gives the following impedance function of the laser diode

$$Z(\omega) = \frac{V(\omega)}{I(\omega)} = R_d \frac{j\frac{\omega}{\tau_s} + \frac{1 + n_{om} - n_e^o}{\tau_s \tau_{ph}}}{-\omega^2 + j\frac{\omega}{\tau_s}\left[n_{ph}^o + 1 + \frac{\tau_s}{\tau_{ph}}\left(1 + n_{om} - n_e^o\right)\right] + \frac{n_{ph}^o + \beta\left[n_e^o\left(1 + 1/n_{ph}^o\right) - n_{om}\right]}{\tau_s \tau_{ph}}} \tag{4}$$

where $V(\omega)$ is the complex amplitude of the junction voltage, $I(\omega)$ is the complex amplitude of the current injected to the laser diode, R_d is the differential resistance of the laser diode, and n_{ph}^o, n_e^o and n_{om} are the normalized steady-state values of N_{ph}^o, N_e^o and N_{om}, respectively $\left(n_{ph}^o = A\tau_s N_{ph}^o, n_e^o = A\tau_{ph} N_e^o \quad and \quad n_{om} A\tau_{ph} N_{om}\right)$. The differential resistance of the laser diode is given by

$$R_d = \frac{2kT}{q}\frac{1}{I_d} \tag{5}$$

where I_d is a normalized current equals to $N_e^o aqd / \tau_s$.

The impedance function of Equation (4) is same as a parallel RLC circuit with a resistor *Rse* in series with the inductor. The obtained intrinsic electrical equivalent circuit of the laser diode is shown in Fig. 1. The values of the components in Fig. 1 are given by

$$R_i = R_d / (n_{ph}^o + 1) \tag{6}$$

$$L_i = R_d \tau_{ph} / \left[\left(n_{ph}^o + \beta\right)\left(n_e^o - n_{om}\right)\right] \approx R_d \tau_{ph} / n_{ph}^o \tag{7}$$

$$C_i = \tau_s / R_d \tag{8}$$

$$R_{se} = \beta R_d \frac{n_e^o}{n_{ph}^o \left(n_{ph}^o + \beta\right)\left(n_e^o - n_{om}\right)} \approx \beta R_d \frac{n_e^o}{\left(n_{ph}^o\right)^2} \tag{9}$$

The resistance R_i including the differential resistance of the laser diode models damping due to the spontaneous and stimulated recombination terms in the rate equations. The resistance R_{se} models damping due to spontaneous emission coupled into the lasing mode. So, damping of the electro-optical resonance is due to the resistances R_i and R_{se}. The capacitance C_i represents the active layer diffusion capacitance of the laser diode. The inductance L_i arises from the small signal analysis of the rate equations and represents the resonance phenomenon of the laser diode with the capacitance C_i.

The resonant frequency of the circuit shown in Fig. 1 is given by

$$f_r = \frac{1}{2\pi} \frac{1}{\sqrt{L_i C_i}} \tag{10}$$

According to Equation (10), it is possible to increase the value of the resonant frequency by decreasing the values of L_i and C_i. Since the values of L_i and C_i are dependent on the laser diode parameters, the resonant frequency can be increased in three ways by

a) decreasing the photon lifetime τ_{ph},

b) increasing the photon density n_{ph}^o,

c) increasing the gain coefficient A, that is, increasing electron density n_e^o.

Putting the values of Li and Ci from Equation (7) and Equation (8) into Equation (10), we get the equation of the relaxation oscillation frequency of the laser diode in terms of the laser diode parameters as

$$f_r = \frac{1}{2\pi} \sqrt{\frac{n_{ph}^o}{\tau_s \tau_{ph}}} \tag{11}$$

Using the normalization constant of the photon density in Equation (11), the equation of relaxation oscillation frequency is found as

$$f_r = \frac{1}{2\pi} \sqrt{\frac{AN_{ph}^o}{\tau_{ph}}} \tag{12}$$

As it can be seen from the above equations that there is a close relationship between the circuit components of the equivalent circuit and the laser diode parameters.

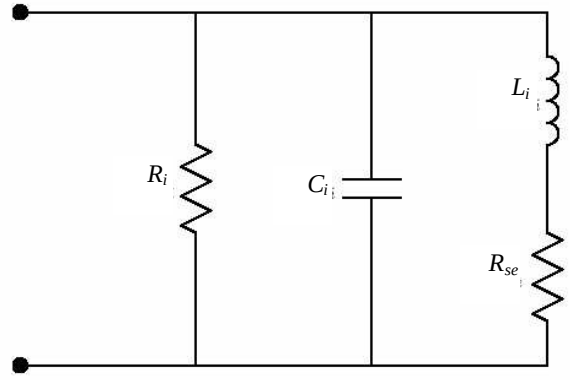

Fig. 1. The intrinsic electrical equivalent circuit of the laser diode.

It is possible to find a slightly different intrinsic electrical equivalent circuit for the laser diode. This is due to fact that the terms which are added to the rate equations for explaining the different phenomena appearing in the light output of the laser diodes and the different geometry lasers will give rise to an intrinsic equivalent circuit which is a slightly different than the circuit shown in Fig. 1. For example, Tucker [6] puts another capacitor parallel to C_i for explaining the space-charge effects in the active region of the laser diode. This capacitance named as the space-charge capacitance, C_{sc}, of the active region. Tucker [6] also uses a non-uniform electron density in his analysis and arrives at an equivalent circuit containing a series resistor, R_{se1}, with the inductor. The equation of C_{sc} is given by

$$C_{SC} = C_{SC(o)}(1 - V/V_D)^{-1/2} \tag{13}$$

where $C_{sc(o)}$ is the zero-bias space-charge capacitance and *VD* is the heterojunction built-in potential which has a value of 1.65 V. The resistance *Rse*1 is given by

$$R_{se1} = \frac{(\Gamma A)^2 \tau_s (N_e^o - N_{om})}{2\left[1 + \left(\frac{2\pi L_{eff}}{W}\right)^2\right]} N_{ph}^o L_i \tag{14}$$

where Γ is the optical confinement factor normal to the junction plane, L_{eff} is the effective carrier diffusion length and *W* is the width of the active layer. As it can be seen from Equation (14), R_{se1} models the lateral carrier diffusion and the optical confinement in the active region. So, the intrinsic electrical equivalent circuit of the laser diode taking into account all the major factors effecting the dynamic response of the laser diode is shown in Fig. 2.

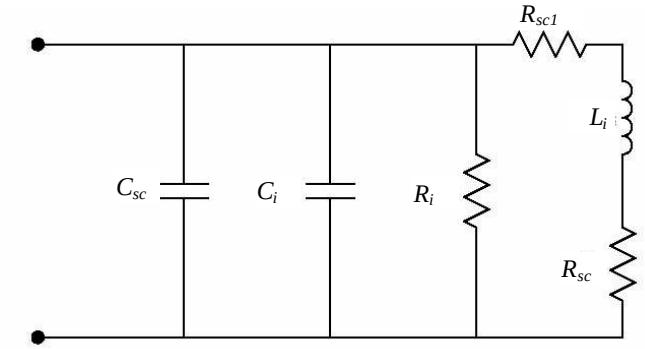

Fig. 2. The complete intrinsic electrical equivalent circuit of the laser diode.

The electrical equivalent circuit of the package and parasitics can easily be found by considering the geometry of the package and the main parasitics elements associated with the laser chip. Since the small-signal ac analysis results in the linearization of the rate equations, the elements of the package and parasitics circuit can directly be added to the intrinsic equivalent circuit of the laser diode. The equivalent circuit of the package and parasitics for BH lasers given by [6] and [7] are similar to each other except that [7] puts and additional series resistance with the parasitic capacitance. Since the package of HLP-3400 laser is exactly same as HLP-1400 laser, we will use the package circuit model of HLP-3400 laser given in [6]. The electrical equivalent circuit of the package and parasitics for BH HLP-1400 laser is shown in Fig. 3. In Fig. 3, L_b is the bond wire inductance, C_m is the shunt package capacitance (ceramic capacitance), R_b is the bond wire resistance, C_p is the parasitic capacitance associated with the laser chip (it is the capacitance between the top and bottom contacts in the area outside the lasing region) and R_c is the contact resistance including the semiconductor bulk resistance. The main contribution to R_c comes from the contacts

because the bulk resistance of semiconductor is very low. For $n = 5\times10^{17}/cm^3$, d = 100 μm, W = 200 μm and l = 300 μm, the bulk resistance of semiconductor is calculated as 7×10^{-2} Ω which is indeed very small.

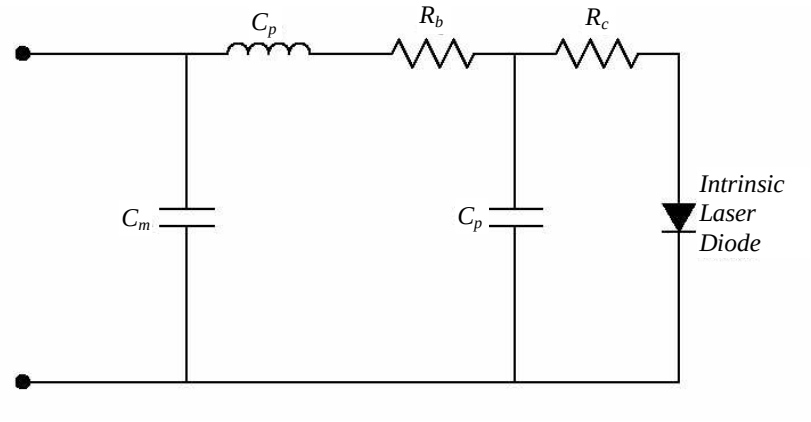

Fig. 3. Electrical equivalent circuit of the package and parasitics.

3. Results

Numerical values of the circuit components including the package parasitics are obtained by computer-aided fitting of the modelled small-signal optical and electrical characteristics to the measured data (microwave s-parameters). In order to find a satisfactory fit at all frequencies the modelled circuit must reasonably be similar to the actual circuit. The intrinsic chip parameters are obtained from the measured small- signal intensity modulation frequency response (microwave *s*- parameter). For BH HLP-3400 model laser diode, Tucker [6] finds the element values of the circuit shown in Fig. 2 at 20 mA injection current as C_{sc} = 10 *pF*, C_i = 380 *pF*, R_i = 1.23 Ω, R_{se1} = 23.4*mΩ*, R_{se} = 34 $\mu\Omega$ and L_s = 7.07 *pH*. According to our S_{11} data, the element values of the same circuit for HLP-1400 model laser diode were found as C_{sc} = 6 *pF*, C_i = 340 *pF*,R_i = 0.84 Ω, R_{se1} = 43*mΩ*, R_{se} = 38 μΩ and L_s = 6.4 *pH* by using the SUPER-COMPACT optimization program. Although we only used s_{11} data of HLP-1400 laser diode which has a different geometry than HLP-3400 laser diode, the results are very close to the values given in [6]. In [7], the typical values of the circuit elements for a AlGaAs laser are given as $R_i \leq 1$ Ω, $C_i \sim 3$ *nF* and $L_i \sim$ *pH*. The value of C_i is much bigger than the value given in [6]. This discrepancy comes from the fact that the elements of the circuit are dependent on the laser parameters which can vary from laser to laser.

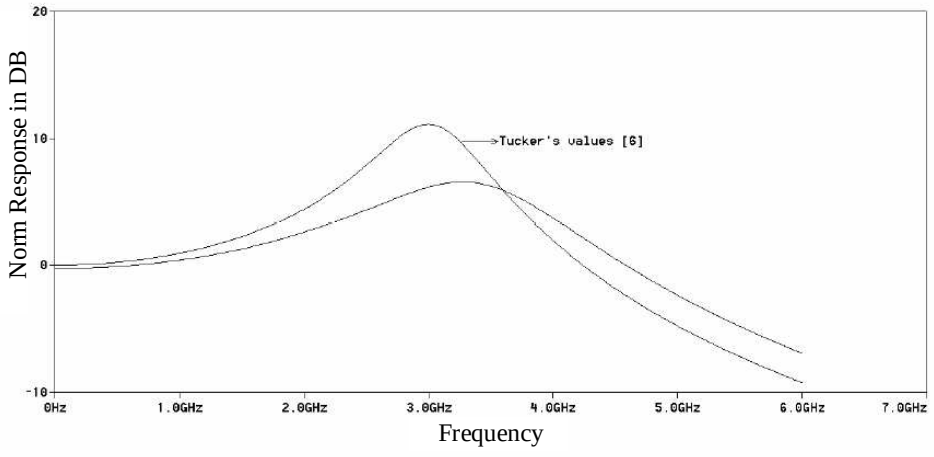

Fig. 4. Comparison of normalized responses of intrinsic equivalent circuits at IDC = 20 mA.

The element values of the circuit shown in Fig. 3 were found in [6] as C_m = 0.29 *pF*, L_b = 1.42*nH*, R_b = 2 Ω, C_p = 14.1 *pF* and R_c = 13.1 Ω. According to our s_{11} parameter of the HLP-1400 laser, we found the element values as C_m = 0.46 *pF*, L_b = 0.54*nH*, R_b = 4.3 Ω, C_p = 0.43 *pF* and R_c = 44 Ω . The discrepancy between our values and the values given in [6] comes from the fact that we didn't use other s-parameters which characterize the circuit. So, a more accurate *S*11 data extending to 20 GHz and also other s-parameters for getting more accurate element values of the complete equivalent circuit are needed.

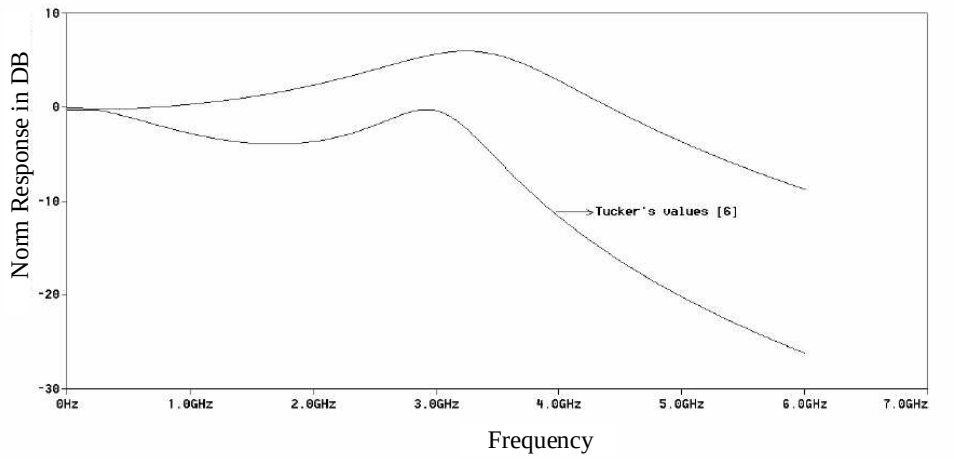

Fig. 5. Comparison of normalized responses of complete equivalent circuits at IDC =20 mA.

PSPICE circuit simulation program which uses the element values found previously is used to find the small-signal intensity modulation response of the intrinsic equivalent circuit. Fig. 4 shows the small-signal intensity modulation response of the intrinsic equivalent circuit upto 6 GHZ at a dc bias value of 25 mA. For comparison, the response of the circuit which uses the Tucker's values [6] is also shown in Fig. 4. The small signal intensity modulation response of the complete electrical equivalent circuit which uses the element values found in this work at dc bias value of 20 mA is also plotted by using PSPICE circuit simulation program. Fig. 5 represents the response of the complete electrical equivalent circuit together with the graph using Tucker's values [6].

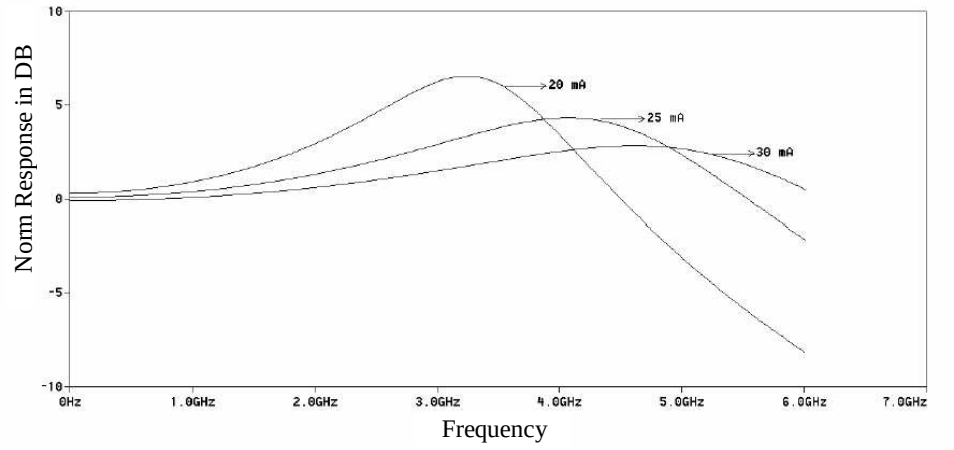

Fig. 6. Normalized response of complete equivalent circuit in DB for three different dc bias value (I_{DC} = 20; 25; 30 mA).

As it can be seen from Fig. 4 and Fig. 5, the response of the circuits increases slightly up to resonance frequency and then decreases rapidly due to the combined effects of the package and

parasitics. As it was explained before, the difference between the graphs shown in Fig. 5 is due to the different geometries of the laser diodes and laser parameters. Fig. 6 shows the response of the complete electrical equivalent circuit at three different dc bias value of 20 mA, 25 mA and 30 mA. As it can be seen from the graphs that the resonance frequency moves to higher frequencies as dc current value increases. This can also be seen from the Equation (10). As dc current increases, electron density increases. This in turn increases the photon density. Hence, the resonance frequency of the circuit increases.

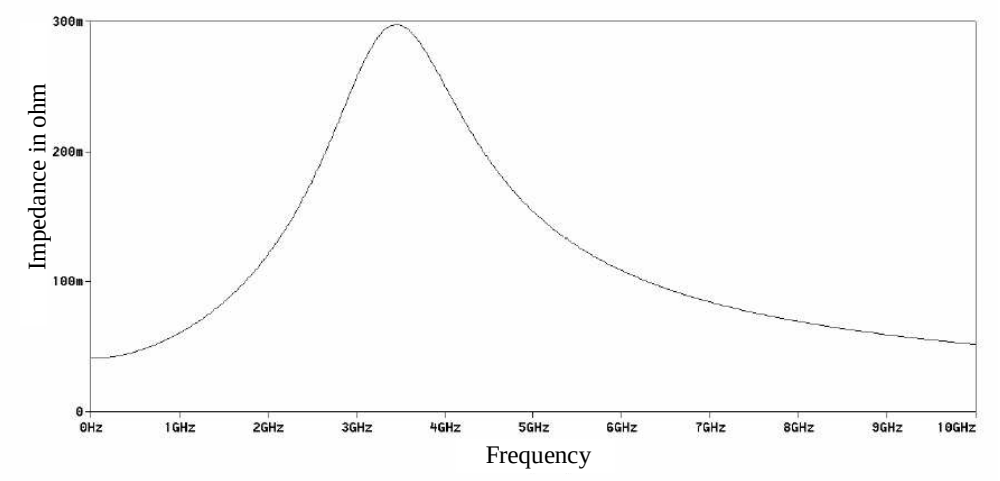

Fig. 7. Impedance of intrinsic equivalent circuit.

Fig. 7 show the impedance of the intrinsic equivalent circuit. The impedance of the intrinsic equivalent circuit is very small at all frequencies except at the resonant frequency. The impedance has a maximum value at the resonant frequency which doesn't exceed 1 Ω. In order to see this, we calculated the impedance of the intrinsic equivalent circuit by using the element values. The resonant frequency of the circuit was calculated as 3.4 GHz from Equation (10). The impedance of the circuit at this frequency 298×10^{-3} - which is much smaller than 1 Ω. At other frequencies, the impedance is much smaller than the above value. So, the impedance of the intrinsic laser diode can be treated as a short circuit (ac short) at all frequencies and furthermore, it has also very small value as compared with the large external parasitics elements. In order to see the effects of the package and parasitics on the impedance of the laser diode, impedance characteristic of the complete equivalent circuit is plotted in Fig. 8.

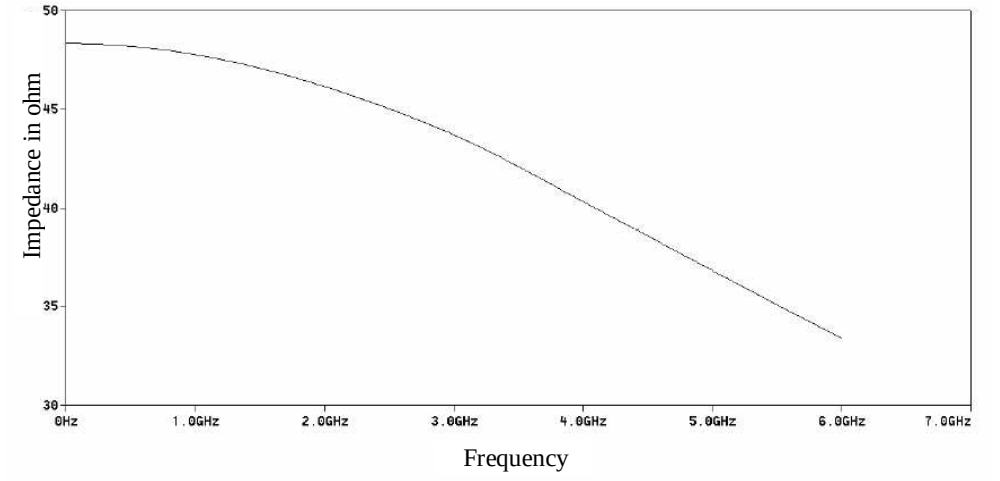

Fig. 8. Impedance of complete equivalent circuit.

As it can be seen from the graph that it is completely different than the impedance characteristic of the intrinsic equivalent circuit. This is expected since the intrinsic circuit has almost zero impedance almost at all frequencies. Therefore, Fig. 8 only shows the impedance of the package and parasitics. At low frequencies it is close to 50 Ω and decreases as frequency increases.

The overall modulation response of the laser diode can be written as

$$H(\omega) = \frac{I(\omega)}{V_s(\omega)} \frac{V_o(\omega)}{I(\omega)} = \eta H_i(\omega) \tag{15}$$

where $H_i(\omega)$ is the response of the intrinsic laser diode, $I(\omega)$ is the current injected to the intrinsic laser diode, $V_s(\omega)$ is the voltage of rf generator, $V_o(\omega)$ is the output voltage representing the modulated light output and η is the injection ratio which is equal to $I(\omega)=Vs(\omega)$. η also represents the admittance of the package and parasitics circuit.

In order to see how η effects the overall modulation response, η must be found. For simplification the capacitance C_m is neglected due to its small value and the intrinsic laser diode is replaced by a short circuit. So, the circuit of Fig. 3 for evaluation of η will look like the circuit shown in Fig. 9. In Fig. 9, R_o represents the characteristic impedance of the transmission line and accounts for the impedance mismatch in the system. *Ro* has a value of 50 - for standard transmission lines. The analysis of the circuits shown in Fig. 9 will give the following equation for η as

$$\eta = \frac{1}{R_c C_p L_b} \frac{1}{(j\omega)^2 + j\omega\left(\frac{L_b + R_c R_o C_p + R_c R_b C_p}{R_c C_p L_b}\right) + \frac{R_c + R_o + R_b}{R_c C_p L_b}} \tag{16}$$

Equation (16) is the equation of a second-order system with the values of ω_o and ζ given as

$$\omega_o = \sqrt{\frac{R_c + R_o + R_b}{R_c C_p L_b}} \tag{17}$$

$$\varsigma = \frac{1}{2}\sqrt{\frac{(L_b + R_c R_o C_p + R_c R_b C_p)^2}{R_c C_p L_b (R_b + R_c + R_o)}} \tag{18}$$

ζ is the damping coefficient of the system and equals to 1=2*Q* where *Q* is the quality factor of the circuit. In the second-order system, if ζ is large (low *Q*) the system did not respond so greatly at ω_b and also response did not drop off so rapidly as the frequency changed from ω_o. This means that there will be no resonance if *Q* of the circuit is small enough. If *Q* of the circuit is high, the circuit will resonate at a frequency of ω_b which can be lower or higher than ω_r dependent on the circuit parameters. Then, it wouldn't be possible to modulate the laser diode with a frequency higher than ω_o due to fact that rf current injected to the laser diode will be zero at the resonance frequency of the package circuit. So, the package and the laser chip causing parasitics must be carefully be designed to ensure that the package circuit will not resonate at w_o. If *Q* of the circuit is small, the current injected to the intrinsic laser diode will be -3 dB lower than its low frequency value at around ω_o. This means that the package and parasitics circuit will not limit the modulation response of the laser diode upto the frequency at least ω_o. After this frequency, there will be a drastic decrease in the modulation response of the laser diode due to decrease of rf current. According to the values given in [6], *Q* of the circuit and f_o are calculated as 0.375 and 2.5 GHz respectively. According to our values, *Q* and f_o of the circuit were found as 0.64 and 15.6 GHz respectively. Since *Q* of the package circuit of HLP-1400 laser diode is small and f_o has a high value, the modulation response of HLP-1400 laser is not limited by the package circuit. This means that decrease in the modulation response of HLP-1400 laser is due to relaxation oscillation.

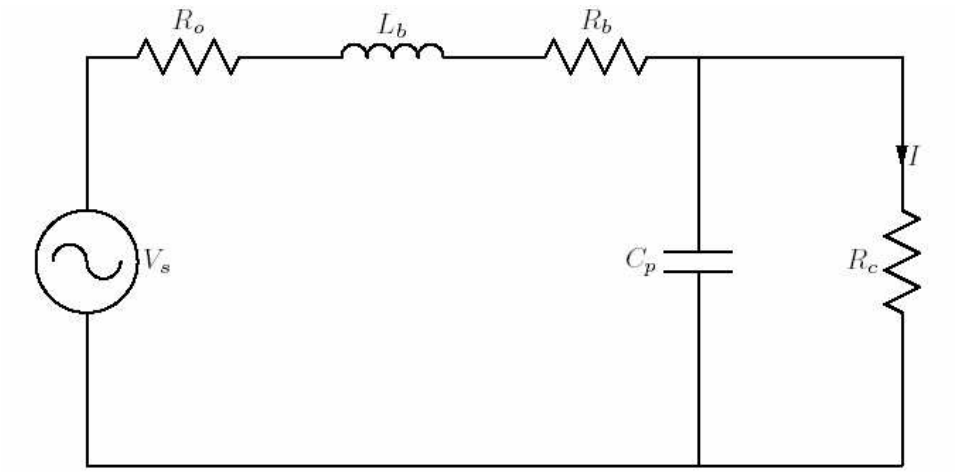

Fig. 9. Circuit for the evaluation of η.

In order to increase the injection ratio, the impedance of the laser diode must be matched to the transmission line. The impedance of the laser diode is not a pure resistance having a value of 3 or 4 Ω as it can be seen from the complete equivalent circuit. S_{11} data shows that the laser diode has a complex impedance varying with frequency. The unmatched impedance will reflect the most part of rf current back into the rf generator. The impedance matching can be achieved by using stub matching technique consisting of a series or a shunt short circuit connected to the transmission line. We will consider the single shunt stub matching for a particular value of the laser impedance at a certain frequency. Although it is no possible to match all values of the load impedance with a single stub, the mathematical analysis of the single stub is much easier than the three stub matching. The input impedance of the transmission line is given by

$$Z_{in} = Z_o \frac{Z_L + jZ_o \tan \gamma l}{Z_o + jZ_L \tan \gamma l} \tag{19}$$

where Z_o is the characteristic impedance of the line, ZL is the complex load impedance, γ is the phase constant and l is the length of the line. For a given value of load impedance and frequency, we can find the location and the length of the stub defined in Fig. 10 by using Equation (19). Writing Equation (19) as an admittance, we get

$$Y_{in} = Y_o \frac{Z_o + jZ_L \tan \gamma l_1}{Z_L + jZ_0 \tan \gamma l_1} = G_{in} + jB_{in} \tag{20}$$

G_{in} and B_{in} are given by

$$G_{in} = \frac{RZ_o(1+\tan^2 \gamma l_1)}{R^2 + (X + Z_o \tan \gamma l_1)^2} \tag{21}$$

$$B_{in} = Y_o \frac{R^2 \tan \gamma l_1 - Z_o(X + Z_o \tan \gamma l_1) + X \tan \gamma l_1 (X + Z_o \tan \gamma l_1)}{R^2 + (X + Z_o \tan \gamma l_1)^2} \tag{22}$$

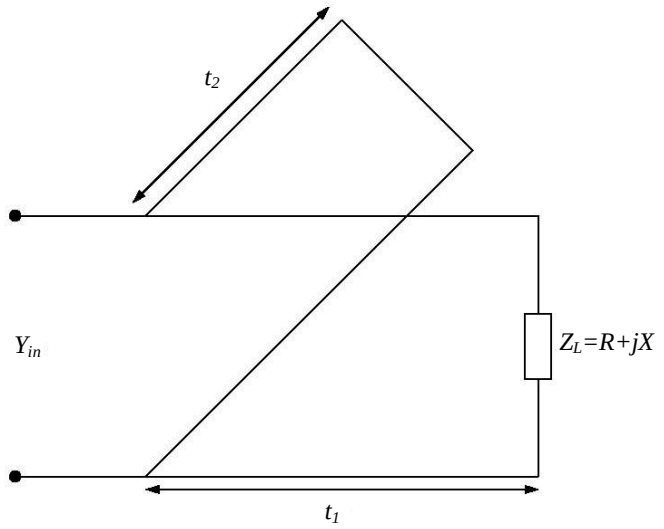

Fig. 10. Definition of the length and the location of the stub.

For impedance matching, $G_{in} = 1/Z_o$ and $|B_{in}| = -|Bsc|$ conditions must be met. From the condition of $G_{in} = 1/Z_o$, we get the location of stub as

$$l_1 = \frac{\lambda_g}{2\pi\gamma}\tan^{-1}\left[\frac{XZ_0 \pm \sqrt{Z_o R(R^2 + X^2 + Z_o^2 - 2RZ_o}}{Z_o(R - Z_0)}\right] \tag{23}$$

where λ_g is the wavelength in the transmission line and equals to $\lambda_0 / \sqrt{\varepsilon_r}$. Since we have trigonometric function, $\pm l_1 \pm \frac{n\lambda_g}{2}$ are also solutions for n = 0*;* 1*;* 2 ... From the condition of $|B_{in}| = -|B_{sc}|j$ where B_{sc} is the suseptance of the short circuit, we get the length of the stub as

$$l_2 = \frac{\lambda_g}{2\pi\gamma} tan^{-1}\left[\frac{R^2 + (X + Z_o \tan\gamma l_1)^2}{\tan\gamma l_1(R^2 - Z_o^2 + X^2) + XZ_o \tan\gamma l_1 - Z_o X}\right] \tag{24}$$

and also $\pm l_2 \pm \frac{n\lambda_g}{2}$ are also solutions for n = 0*;* 1*;* 2 ... For Z_L = 5 + *j50* **Ω** at f = 1.15 GHz,, the values of l_1 and l_2 are found as 2.7 cm and 4.28 cm, respectively, by using Equation (23) and Equation (24). Since the stub location is not much close to the load impedance, a slight change in frequency will lead to unmatched condition. Single stub matching is very sensitive to slight frequency changes and will not match all values of the load impedance. A three stub matching which can match all values of the load impedance must be used.

4. Conclusions

The electrical equivalent circuit of the package and parasitics is obtained by considering the geometry of the package and the main parasitics elements associated with the laser chip. Numerical values of the circuit components including the package and parasitics components are obtained by computer aided fitting of the modelled small signal optical and electrical characteristics to the measured microwave s-parameters data. In order to find a satisfactory fit at all frequencies the

modelled circuit must reasonably be similar to the actual circuit. The component values obtained for HLP-1400 laser diode is similar to the other model laser diodes (HLP-3400) manufactured by Hitachi. The small discrepancy comes from the fact that the elements of the circuit are dependent on the laser parameters and the package which can vary from laser to laser.

References

[1] K. Hagimoto, N. Ohta, K. Nakagawa, Electron. Lett. **18**, 796 (1982).
[2] K. Y. Lau, N. Bar-Chaim, I. Ury, C. H. Harder, A.Yariv, Appl. Phys. Lett. **43**, 1 (1983).
[3] H. Kressel., Ed., Semiconductor Devices for Optical Communications, Topics in Applied Physics, 39, New York: Springer-Verlag (1980).
[4] R. A. Kiehl, D. M. Drury, IEEE Trans. Microwave Theory Tech. **MTT-29**, 1004 (1981).
[5] R. Tucker, D. J. Pope, IEEE Trans. Microwave Theory Tech. **MTT-31**, 289 (1983).
[6] R. Tucker, D. J. Pope, IEEE J. Quantum Electron. **QE-19**, 1179 (1983).
[7] J. Katz, S. Margalit, C. Harder, D. Wilt, A. Yariv, IEEE J. Quantum Electron. **QE-17**, 4 (1981).
[8] R. Tucker, J. Lightwave Tech.**LT-3**, 1180 (1985).
[9] W. Chen and S. Liu, IEEE J. Quantum Electron. **QE-36**, 2128 (1996).
[10] D. S. Gao, S. M. Kang, R. P. Bryan, J. J. Coleman, IEEE J. Quantum Electron. **QE-26**, 1206 (1990).
[11] S. C. Kan, K. Y. Lau, IEEE Photonics Tech. Lett. **4**, 528 (1992).
[12] M. F. Lu, J. S. Deng, C. Juang, M. J. Jou, B. J. Lee, IEEE J. Quantum Electron. **QE-31**, 1418 (1995).
[13] B. P. C. Tsou, D. L. Pulfrey, IEEE J. Quantum Electron. **QE-33**, 246 (1997).
[14] P. V. Mena, S. Kang, T. A. DeTemple, J. Lightwave Tech. **LT-15**, 717 (1997).
[15] I. Esquivias, S Weisser, B. Romero, J. D. Ralston, J. Rosenzweig, IEEE J. Quantum Electron. **QE-35**, 635 (1999).